

Searching for Candidates of Orbital Decays among Transit Exoplanets

Li-Chin Yeh^a, Ing-Guey Jiang^{b,c}, Napaporn A-thano^b

^a*Institute of Computational and Modeling Science, National Tsing-Hua University, Hsin-Chu, Taiwan*

^b*Department of Physics and Institute of Astronomy, National Tsing-Hua University, Hsin-Chu, Taiwan*

^c*Center for Informatics and Computation in Astronomy, National Tsing-Hua University, Hsin-Chu, Taiwan*

Abstract

Transit observations have become an important technique to probe exoplanets. Therefore, there are many projects carrying on organized observations of transit events, which make a huge amount of light-curve and transit timing data available. We consider this as an excellent opportunity to search for possible orbital decays of exoplanets from this big number of mid-transit times through data-model fitting with both fixed-orbit and orbit-decay models. In order to perform this task, we collect mid-transit-time data from several sources and construct the most complete database up to date. Among 144 hot Jupiters in our study, HAT-P-51b, HAT-P-53b, TrES-5b, WASP-12b are classified as the orbit-decay cases. Thus, in addition to reconfirming WASP-12b as an orbit-decay planet, our results indicate that HAT-P-51b, HAT-P-53b, TrES-5b are potential orbit-decay candidates.

Keywords: exoplanets, planet-star interactions

1. Introduction

It is well known that transit observations have made significant contribution to the discoveries of extra-solar planets (exoplanets). With the transit method, ground-based telescopes were employed to do sky surveys and brought a chain of exoplanet detections (Alonso et al., 2004; Bakos et al., 2004; Pollacco et al., 2006). Through the same method, space telescopes such as CoRoT (Convection, Rotation and planetary Transits), Kepler, Transiting Exoplanet Survey Satellite (TESS) also joined this journey of discoveries (Auvergne et al., 2009; Borucki et al., 2010; Barclay et al., 2018).

Because (a) the transit probability is higher for those planets closer to the host stars; (b) the transit event happens more frequently for planets with shorter orbital periods; (c) the transit depth is larger if the planet size is bigger relatively to the host star, a huge number of hot Jupiters have been detected. As these hot Jupiters are so close to their host stars, theoretically, these planets might experience tidal orbital decay (Jiang et al., 2003) or lose their masses through the mass transfer into Roche lobes (Valsecchi et al., 2015; Jackson et al., 2016).

In order to further constrain the orbital parameters, and study the above theoretically predicted orbital decay or mass loss, these discovered exoplanets' transit events at later epochs have been monitored through many following-up observations intensively. For example, Winn et al. (2009) performed two transit observations of the exoplanet WASP-4b. Their work led to the updated planetary mass and radius. They found that this planet was 15% larger than expected and was thus a bloated planet. Jiang et al. (2013) presented five transit light curves of TrES-3b and proposed that there could be a possible transit timing varia-

tion (TTV) for this planet. Mannaday et al. (2020) further studied this system and reconfirmed this possibility. In addition, the possible orbital decay of WASP-43b (Hellier et al., 2011) was also investigated, and both positive and negative results were claimed controversially (Blecic et al., 2014; Jiang et al., 2016; Hoyer et al., 2016; Davoudi et al., 2021; Garai et al., 2021).

Interestingly, Bouma et al. (2019) later employed 18 TESS transit light curves of WASP-4b and discovered that the transits occurred earlier than previously predicted. They concluded that the orbital period of WASP-4b was changing, which could be caused by tidal orbital decay, apsidal precession, or the gravitational influence of a third body (Miralda-Escudé, 2002; A-thano et al., 2022).

In fact, TTV has also become one of the tools to detect new exoplanets. For example, a further analysis on transit timing data by Sun et al. (2019) led to the discoveries of additional two new exoplanets in Kepler-411 system, which was previously known to host two transiting planets. Moreover, Barros et al. (2022) employed 12 transit light curves to investigate the tidal deformation of WASP-103b and Szabó et al. (2022) found large-amplitude TTVs of AU Microcopii b and c through combined TESS and CHEOPS transit data.

Finally, Maciejewski et al. (2016) and Patra et al. (2017) collected mid-transit times of the exoplanet WASP-12b and confirmed the TTV of WASP-12b. They favored the model of orbital decay and a decay rate of -25.60 ± 4.0 ms per year was reported. Further timing analysis (Yee et al., 2020; Turner et al., 2021; Wong et al., 2022) supports that the orbit of WASP-12b is decaying.

On the other hand, the huge amount of light curves obtained by the Kepler Space Telescope leads to an excellent database of mid-transit times, which triggers many further studies. For example, Ford et al. (2012) searched for TTVs from the first four-

Email address: jiang@phys.nthu.edu.tw (Ing-Guey Jiang)

month Kepler data and studied multi-planet systems. Steffen et al. (2012) used statistics tests to search for TTVs among pairs of Kepler Object of Interest (KOI) in multi-transiting systems. Finally, Holczer et al. (2016) presented a transit timing catalog of 2599 KOIs and showed clear TTVs among many multi-planet systems. Recently, these Kepler transit timing data were employed by Wu et al. (2023) to search for hidden nearby companions to hot Jupiters through examining TTV signals, and also used by Kipping and Yahalomi (2023) to search for exomoons.

In order to provide a platform to give information of transit events and collect transit light curves, Exoplanet Transit Database (ETD) was established (Poddany et al., 2010). It allows both amateur and professional astronomers to upload transit light curves. It employs an analytic model to determine mid-transit times. The predicted information of coming transit events, the observational data of transit light curves, and values of mid-transit times are all publicly available from ETD website. Hagey et al. (2022) then took ETD mid-transit times and searched for long-term period variations. In addition, with a goal to constrain the future observational timing of proposed targets of ARIEL space telescope (Pascale et al., 2018), Kokori et al. (2021) organized the ExoClock project which builds a big network of telescopes and obtain many exoplanet transit light curves. The ExoClock project also provides an interactive platform that light curves can be uploaded by observers and become publicly available. Kokori et al. (2022) updated their telescope capabilities and reported their results of ephemerides of 180 planets. Recently, Kokori et al. (2023) further present a homogenous catalog of updated ephemerides for 450 planets. The main objective of ExoClock is to continuously improve the precision of exoplanet ephemerides. After more mid-transit times are collected, the slope of the linear ephemerides is likely to be changed and the future transit timing would be drifted (Kokori et al., 2022). However, if a linear function is still the best model for mid-transit times at different epoch, there is no TTV. The TTV could be confirmed to exist only when a non-linear model of mid-transit time gives a better fitting than linear models.

Moreover, Ivshina and Winn (2022) provided a database of transit times of 382 planets derived from TESS data. With these huge amount of collected mid-transit-time data, it is a good opportunity to search for possible orbital decays of hot Jupiters through data-model fitting. In this paper, we collect all mid-transit times from Holczer et al. (2016), Ivshina and Winn (2022), Kokori et al. (2023) and focus on examining whether there are any suspected on-going orbital decays among transit hot-Jupiter planets.

Therefore, we would firstly select hot Jupiters from all planets in these three catalogs. After data-model fitting, these hot Jupiters would be classified into several types based on the results of TTV analysis. Among these, the most important planets are those belong to the orbit-decay-TTV type. With best-fit models, their values of stellar dissipation parameters or orbital evolution would be determined. This paper is organized as follows. §2 describes the mid-transit-time data and planet samples. §3 describes the process of data-model fitting and presents the classification. §4 provides theoretical models and interpre-

tations of the orbit-decay cases. §5 makes conclusions.

2. The Mid-Transit-Time Data and Hot-Jupiter Samples

In this paper, the mid-transit-time data from Holczer et al. (2016) (Kepler Catalog), Ivshina and Winn (2022) (TESS Catalog), and Kokori et al. (2023) (ExoClock Catalog) are all collected. There are totally 2430 planets and the majority is from the Kepler Catalog. In order to estimate tidal dissipation parameters and determine the orbital evolution, we focus on those exoplanets with known values of mass in this paper and leave those exoplanets with unknown values of mass to be studied in the future. After examining the Extrasolar Planets Encyclopaedia (<http://exoplanet.eu/>), only 700 out of these 2430 planets have the values of mass (m) and orbital period (p). Fig. 1 shows the distribution of these 700 planets on the $p - m$ plane. After employing the definition of hot Jupiter (Zhu and Wu, 2018), i.e. $p < 10$ (days) and $m > 0.3$ Jupiter-Mass, 390 planets are selected in the top-left corner of Fig. 1 as indicated by the dashed lines.

In addition, for a particular planet, when there are more than one mid-transit-time data for the same transit epoch, we take the weighted mean to get the mid-transit time and the corresponding uncertainty for that epoch. In order to have sufficient mid-transit-time data points for further analysis, only those planets with 10 or more mid-transit times are included in our study. Thus, only 309 out of 390 hot Jupiters will be taken to do the data-model fitting presented in the next section.

3. The Classification

Our goal is to examine whether there are any TTVs among the selected planets, i.e. hot Jupiters, in the data, and whether these TTVs imply orbital decays. The minimization of chi-square functions would be performed and the corresponding reduced chi-square of best-fit models would be used as an indicator of good or bad fittings. This is because the value of reduced chi-square is usually less than ten and its meaning can be easily understood as an averaged weighted square of data-model differences. In addition, the Bayesian Information Criterion (BIC) would be employed during the process of selecting orbit-decay cases.

Based on these fitting results, exoplanets are classified into different categories. We shall be aware that these calculations are based on statistics and we regard these results as likely tendencies with certain probabilities.

3.1. The Data-Model Fitting

For each planet, two analytic models would be employed to fit the mid-transit time data through the emcee package (Foreman-Mackey et al., 2013), which is an implementation of Goodman & Weare's Affine Invariant Markov Chain Monte Carlo (MCMC) algorithm (Goodman and Weare, 2010). With the values of reduced chi-square of two different fitting models, we are able to classify these exoplanets into three categories,

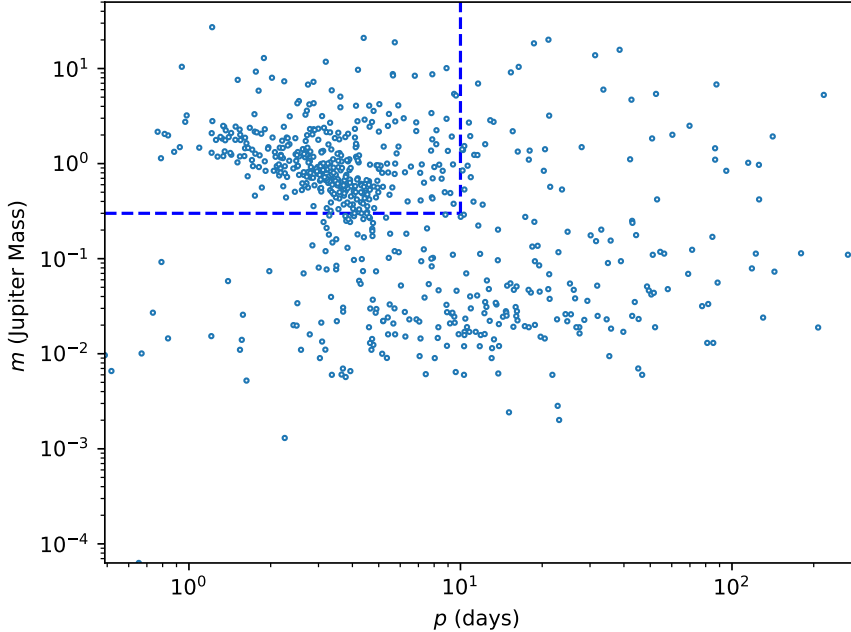


Figure 1: The distribution of 700 planets on the $p - m$ plane. The dashed lines indicate the conditions of hot Jupiters.

i.e. the unclassified-TTV type, the null-TTV type, and the orbit-decay-TTV type. The classification rule would be described in the later part of this subsection.

The first model corresponds to a fixed orbit with a constant orbital period, so the mid-transit time is a linear function of transit number. That is

$$t_{tra}(N) = t_f + P_f N, \quad (1)$$

where t_{tra} is the mid-transit time as a function of N , N is the transit number, t_f is a reference time, and P_f is the orbital period. There are two fitting parameters, t_f and P_f , so the degree of freedom is the number of data point minus two for this model. After the data-model fitting process, we would obtain the best-fit t_f and P_f and the corresponding chi-square χ_f^2 . The value of reduced chi-square $R\chi_f^2$ is then calculated as the chi-square divided by the degree of freedom. Through the MCMC sampling of data-model fitting, the posterior probability distribution of fitting parameters can be obtained. Following Hogg and Craig (1989) and using the standard deviation (σ) of a normal distribution as the parameter uncertainty, the 15.9 percentile and 84.1 percentile of a posterior probability distribution are set as the uncertainty boundaries for all fitting parameters in this paper.

However, when the orbit of an exoplanet changes slowly, the first derivative of period with respect to N will not be zero and the mid-transit time will be slightly shorter or longer for each epoch. In this case, an exoplanet will drift inward or outward slightly every epoch. It is therefore worthwhile to consider a second model with more terms to include possible orbital variations.

The second model is the one allows possible orbital variations (Patra et al., 2017; Su et al., 2021) and the mid-transit time t_{tra} is a quadratic function of transit number N . That is

$$t_{tra}(N) = t_v + P_v N + \frac{1}{2} \frac{dP_v}{dN} N^2, \quad (2)$$

where dP_v/dN is the period derivative with respect to N . There are three parameters, t_v , P_v , and dP_v/dN . The degree of freedom is the number of data point minus three in this model. After the MCMC process, we will obtain the best-fit t_v , P_v , dP_v/dN , the chi-square's value χ_v^2 , and also the reduce chi-square's value which is denoted as $R\chi_v^2$.

Please note that because we decide to focus on the orbital decays, we only consider those planets with the best-fit $dP_v/dN < 0$. After removing 165 planets with best-fit $dP_v/dN \geq 0$, we finally have 144 hot Jupiters as our samples in this paper.

The values of best-fit reduced chi-square for above two models will be determined for all 144 hot Jupiters, and thus all considered hot Jupiters have their own $R\chi_f^2$ and $R\chi_v^2$. When both best-fit reduced chi-square have values larger than or equal to 3.0, i.e. $R\chi_f^2 \geq 3$ and $R\chi_v^2 \geq 3$, it means neither the fixed-orbit model nor orbit-decay model could fit the data well. Thus, it indicates that, for this considered exoplanet, there are some level of TTV but the data might not closely follow the prediction of our orbit-decay model. In this case, it is set to be the unclassified-TTV type.

For the rest of hot Jupiters, we need to determine whether they belong to the null-TTV type or the orbit-decay-TTV type. Because the BIC has been the choice of methods used to pick up the better model in literature (Patra et al., 2017; Mannaday et al., 2022; Hagey et al., 2022), we will calculate BIC values

of both fixed-orbit model and orbit-decay model of a given hot Jupiter. Once BIC values of two models are obtained, the standard way is to pick up the one with smaller BIC value as the preferred model implied by the data. However, the BIC values of two models could be very close for some cases, it is better to estimate the uncertainties of BIC values through the bootstrap method (Press et al., 1992; Jiang et al., 2007), in which the BIC values are calculated for a large number of independent repetitions of bootstrap sampling.

Thus, for those planets with $R\chi_f^2 < 3$ or $R\chi_v^2 < 3$, we calculate the BIC values (Patra et al., 2017; Mannaday et al., 2022; Hagey et al., 2022) of the fixed-orbit model BIC_f and the orbit-decay model BIC_v as,

$$\begin{aligned} BIC_f &= \chi_f^2 + k \log(n_m) \\ BIC_v &= \chi_v^2 + k \log(n_m), \end{aligned} \quad (3)$$

where χ_f^2 is the chi-square value of fixed-orbit model, χ_v^2 is the chi-square value of orbit-decay model, n_m is the number of mid-transit-time data, and k is the number of free parameters. Here $k=2$ for the fixed-orbit model, and $k=3$ for the orbit-decay model.

In order to estimate the uncertainties of BIC_f and BIC_v , the bootstrap sampling is performed for 2000 times (Jiang et al., 2007) and the 25, 50, 75 percentile values are determined. The confidence intervals (BIC_{f25}, BIC_{f75}) and (BIC_{v25}, BIC_{v75}) are then obtained. We set the planets with $BIC_{v75} < BIC_{f25}$ as the orbit-decay-TTV type, and assign the rest to be the null-TTV type.

3.2. The Unclassified-TTV Type

After performing the above tasks, the classification can be done. There are 22 planets belonging to the unclassified-TTV type as listed in Table 1. Their values of $R\chi_f^2$, $R\chi_v^2$, and the number of mid-transit-time data are presented in Table 1.

The orbital properties of these systems being listed in the unclassified-TTV type are not completely clear yet. They deserve future further investigations.

3.3. The Orbit-Decay-TTV Type

After the bootstrap sampling, the histograms of BIC values of all those planets not in unclassified-TTV type are obtained and their corresponding confidence intervals (BIC_{f25}, BIC_{f75}) and (BIC_{v25}, BIC_{v75}) are then determined. Fig. 2 presented the BIC histograms of four planets with $BIC_{v75} < BIC_{f25}$. Their BIC values of orbit-decay model are smaller than the values of fixed-orbit model at the 75% confidence level. Thus, they are set as the orbit-decay-TTV type.

In Table 2, the names of planets, the values of $R\chi_f^2$, $R\chi_v^2$, the best-fit parameters P_v , t_v , dP_v/dN , and the number of mid-transit-time data are listed.

In Fig. 3, the O-C diagrams of those planets being the orbit-decay-TTV type are presented. Both HAT-P-51b and HAT-P-53b were discovered by Hartman et al. (2015). HAT-P-51b is a 0.309 Jupiter-Mass planet with orbital period 4.2 days while HAT-P-53b is a 1.487 Jupiter-Mass planet with orbital period 1.96 days. TrES-5b was discovered by Mandushev et al. (2011).

It is a hot Jupiter with mass 1.778 Jupiter-Mass and an orbital period 1.48 days. WASP-12b is a 1.47 Jupiter-Mass planet with orbital period 1.09 days. It is a best-known orbit-decay exoplanet. According to our best-fit values of dP_v/dN , HAT-P-53b, TrES-5b, and WASP-12b have similar order of orbit-decay rates but HAT-P-51b has a larger orbit-decay rate. Their star-planet tidal interactions and the corresponding dissipation parameters will be further discussed in the next section.

3.4. The Null-TTV Type

For the null-TTV type, there are 118 planets. The values of $R\chi_f^2$, $R\chi_v^2$, the best-fit values of P_f , t_f in Eq. (1), which lead to new ephemerides, and the number of mid-transit-time data are presented in Table 3.

4. The Systems with Orbital Decays

In order to investigate the physics of orbital evolution of the star-planet systems with orbital decays, theoretical models of orbital decays are described here. Following Goldreich and Soter (1966), Jackson et al. (2008), and Murray and Dermott (1999), the orbital evolution of a planet influenced by the tidal effect can be described as

$$\begin{aligned} \frac{1}{a} \frac{da}{dt} &= - \left[\frac{63}{2} (GM_*^3)^{1/2} \frac{R_p^5}{Q_p M_p} e^2 \right] a^{-13/2} \\ &\quad + \text{sign}(\Omega - n) \frac{9}{2} \left(\frac{G}{M_*} \right)^{1/2} \frac{R_*^5 M_p}{Q_*} a^{-13/2}, \quad (4) \\ \frac{1}{e} \frac{de}{dt} &= - \left[\frac{63}{4} (GM_*^3)^{1/2} \frac{R_p^5}{Q_p M_p} \right] a^{-13/2} \\ &\quad + \text{sign}(2\Omega - 3n) \frac{171}{16} \left(\frac{G}{M_*} \right)^{1/2} \frac{R_*^5 M_p}{Q_*} a^{-13/2}, \quad (5) \end{aligned}$$

where a is the orbital semi-major axis, e is the orbital eccentricity, t is the time, G is the gravitational constant, R is a body's radius, M its mass and Q its tidal dissipation parameter, and subscripts p and * refer to the planet and star, respectively. In addition, Ω is the axial angular velocity of star and n is the mean motion of the planet. These two equations determine the time derivatives of orbital semi-major axis and eccentricity. For the case that orbital eccentricity is not equal to zero, the above two equations are coupled and need to be solved simultaneously. For the case of circular orbits, i.e. eccentricity $e = 0$, only the 2nd term of Eq.(4) needs to be considered. To solve the above equations numerically, some planetary and stellar parameters are needed and thus listed in Table 4 for convenience.

4.1. The Planets with Circular Orbits

Among four orbit-decay cases, TrES-5b and WASP-12b are those two planets moving on circular orbits. Under the assumption that $e = 0$ and $\Omega < n$ (Penev et al., 2018; Matsumura et al., 2010), from Eq.(4), we have

$$\frac{da}{dt} = - \frac{9}{2} \left(\frac{G}{M_*} \right)^{1/2} \frac{R_*^5 M_p}{Q_*} a^{-11/2}. \quad (6)$$

Name	$R\chi_f^2$	$R\chi_v^2$	n_m	Name	$R\chi_f^2$	$R\chi_v^2$	n_m
CoRoT-11b	11.10	11.05	22	WASP-16b	4.67	4.33	26
CoRoT-2b	61.45	58.45	138	WASP-19b	4.64	4.27	145
HAT-P-16b	3.42	3.44	47	WASP-2b	4.37	4.43	61
HAT-P-29b	9.66	10.04	20	WASP-33b	8.04	8.35	29
HAT-P-54b	4.09	4.15	64	WASP-41b	3.76	3.87	39
K2-237b	4.69	4.71	35	WASP-45b	11.31	11.02	32
KELT-10b	4.02	3.17	11	WASP-48b	4.06	4.09	111
KELT-25b	5.33	4.99	14	WASP-56b	6.50	5.63	21
KELT-4Ab	5.16	5.32	25	WASP-80b	4.47	4.07	32
TrES-1b	4.06	3.42	81	XO-3b	6.60	3.27	48
WASP-10b	5.73	5.02	74	XO-4b	3.81	3.62	34

Table 1: The values of $R\chi_f^2$, $R\chi_v^2$, and the number of mid-transit-time data of those planets belonging to the unclassified-TTV type.

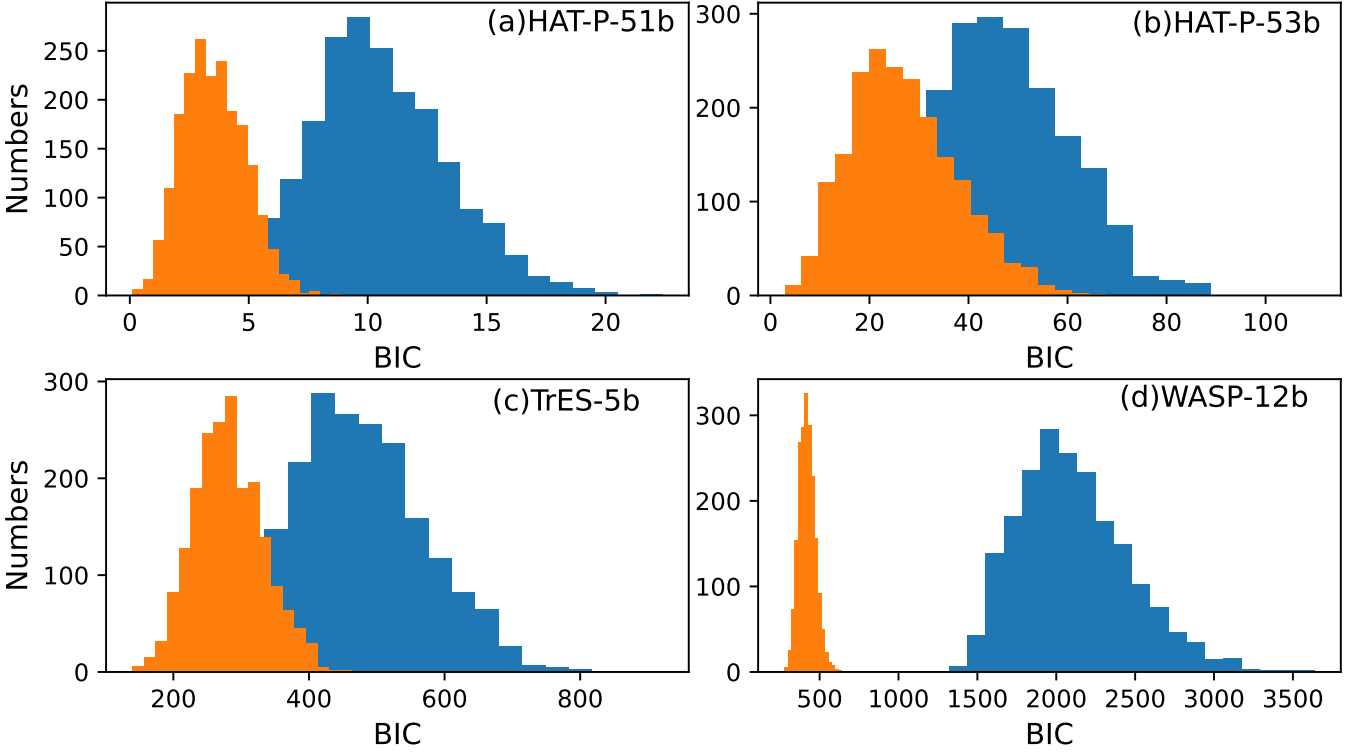


Figure 2: The histograms of BIC values for the four planets being the orbit-decay-TTV type. The BIC values of the fixed-orbit model are in blue color, and the BIC values of the orbit-decay model are in orange color.

Name	$R\chi_f^2$	$R\chi_v^2$	P_v (days)	t_v (BJD)	dP_v/dN	n_m
HAT-P-51b	1.31	0.50	$4.218028 \pm 3 \times 10^{-6}$	2456194.1228 ± 0.0004	$-1.80 \times 10^{-8} \pm 7 \times 10^{-9}$	10
HAT-P-53b	3.10	1.92	$1.961628 \pm 1 \times 10^{-6}$	2455829.4483 ± 0.0004	$-5.1 \times 10^{-9} \pm 1 \times 10^{-9}$	17
TrES-5b	4.60	2.75	$1.4822490 \pm 2 \times 10^{-7}$	2455152.7316 ± 0.0001	$-1.5 \times 10^{-9} \pm 1 \times 10^{-10}$	105
WASP-12b	7.46	1.50	$1.09142185 \pm 7 \times 10^{-8}$	$2454508.97693 \pm 7 \times 10^{-5}$	$-1.05 \times 10^{-9} \pm 3 \times 10^{-11}$	283

Table 2: The values of $R\chi_f^2$, $R\chi_v^2$, the best-fit parameters of the orbit-decay model, and the number of mid-transit-time data of four planets belonging to the orbit-decay-TTV type.

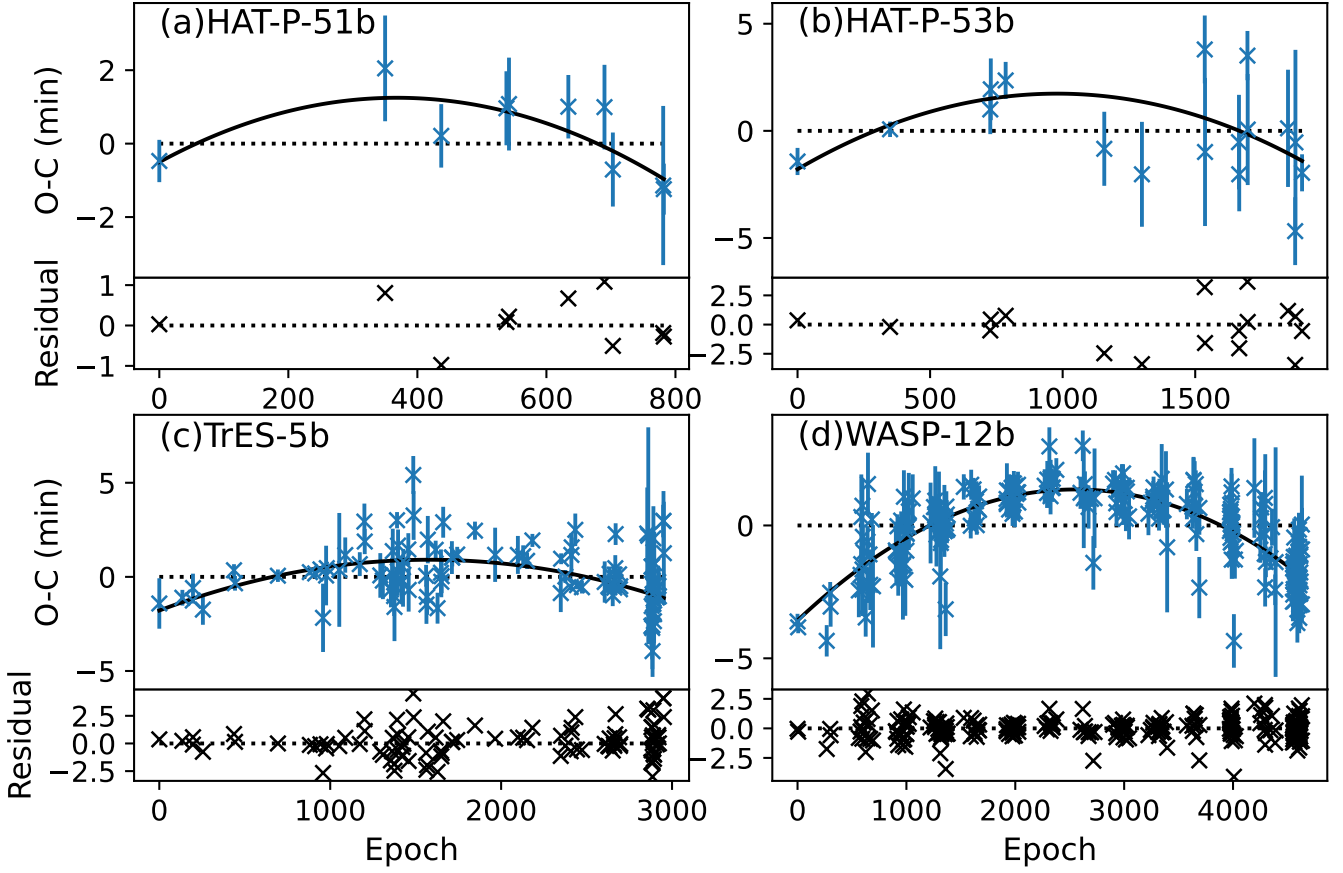


Figure 3: The O-C diagrams of four planets belonging to the orbit-decay-TTV type

Name	$R\chi_f^2$	$R\chi_v^2$	P_f (days)	t_f (BJD)	n_m
CoRoT-19b	0.97	0.99	$3.897138 \pm 2 \times 10^{-6}$	2455261.3388 ± 0.0005	19
CoRoT-5b	0.27	0.27	$4.037916 \pm 1 \times 10^{-6}$	2454400.1990 ± 0.0002	34
EPIC246851721b	1.89	2.01	$6.180268 \pm 2 \times 10^{-6}$	2457828.0285 ± 0.0002	17
HAT-P-1b	1.34	1.27	$4.4652991 \pm 4 \times 10^{-7}$	2453979.9322 ± 0.0002	25
HAT-P-13b	2.20	2.25	$2.9162426 \pm 4 \times 10^{-7}$	2454581.6256 ± 0.0002	47
HAT-P-2b	1.32	1.41	$5.6334686 \pm 5 \times 10^{-7}$	2454212.8566 ± 0.0004	14
HAT-P-22b	1.71	1.63	$3.2122321 \pm 2 \times 10^{-7}$	2454930.2212 ± 0.0002	47
HAT-P-23b	1.51	1.53	$1.21288643 \pm 5 \times 10^{-8}$	2454632.7329 ± 0.0001	79
HAT-P-24b	1.70	1.69	$3.3552444 \pm 2 \times 10^{-7}$	2455206.9115 ± 0.0002	42
HAT-P-25b	1.63	1.58	$3.6528152 \pm 3 \times 10^{-7}$	2455136.6717 ± 0.0002	46
HAT-P-27b	1.44	1.31	$3.0395780 \pm 2 \times 10^{-7}$	2455186.0203 ± 0.0002	24
.....
XO-7b	1.45	1.47	$2.86413530 \pm 8 \times 10^{-7}$	2457917.4754 ± 0.0003	47

Table 3: The values of $R\chi_f^2$, $R\chi_v^2$, the best-fit parameters of the fixed-orbit model, and the number of mid-transit-time data of those planets belonging to the null-TTV type. This table is available in its entirety in machine-readable form. A portion is shown here for guidance regarding its form and content.

Since the orbital period P_v satisfies $P_v^2 = 4\pi^2 a^3/\mu$ and $\mu = G(M_* + M_p) \sim GM_*$, we substitute this relation into Eq.(6) and have

$$\frac{1}{P_v} \frac{dP_v}{dN} = \frac{dP_v}{dt} = \frac{3\pi}{\sqrt{GM_*}} a^{1/2} \frac{da}{dt} = -\frac{27\pi}{2Q_*} \left(\frac{M_p}{M_*}\right) \left(\frac{R_*}{a}\right)^5. \quad (7)$$

The above equation, i.e. Eq.(7), gives the relation between Q_* and dP_v/dN . This relation enables us to estimate the stellar dissipation parameter Q_* from transit observations. In principle, Q_* is inversely proportional to $|dP_v/dN|$.

The data-model fitting in the previous section leads to the best-fit dP_v/dN and also the posterior distribution of dP_v/dN . The best-fit values of Q_* are obtained and shown at the 2nd column of Table 5. In addition, using the 2.3 and 97.7 percentile values (i.e. 2σ) of the posterior distribution of dP_v/dN , the lower limit and upper limit of Q_* are also obtained and shown at the 3rd and 4th column of Table 5. They are denoted as LQ_* and UQ_* .

The result here that TrES-5b being the orbit-decay-TTV type is actually consistent with several previous studies. For example, Sokov et al. (2018) proposed the possible existence of an additional planet in order to explain the detected TTV. Maciejewski et al. (2021) revisited this system by providing more transit light curves. They did not confirm the existence of additional planet, but concluded that the orbital period of TrES-5b could vary on a long timescale. Employing ETD data, Hagey et al. (2022) gave a list of systems, including TrES-5b, which have deviations from a constant orbital period. Our best-fit Q_* is around 10^4 which is close to the lower end of the suggested range in Matsumura et al. (2010).

WASP-12b is a well-known confirmed orbit-decay case (Patra et al., 2017). From Table 5, the value of Q_* is about 1.65×10^5 . Previously, Patra et al. (2017) estimated Q_* to be about 2×10^5 and Maciejewski et al. (2018) reported a value of $Q_* = (1.82 \pm 0.32) \times 10^5$. Thus, our result is consistent with previous results and we here reconfirm this orbit-decay case.

4.2. The Planets with Eccentric Orbits

As shown in Penev et al. (2018); Matsumura et al. (2010), the stellar spins are usually slower than the orbital motion of hot Jupiters, we thus assume that the axial angular velocity of star is smaller than the mean motion of the planet, i.e. $\Omega < n$. From Eq.(4) and Eq.(5), we have

$$\begin{aligned} \frac{1}{a} \frac{da}{dt} &= -\frac{63}{2} (GM_*^3)^{1/2} \frac{R_p^5}{Q_p M_p} e^2 a^{-13/2} \\ &\quad + \frac{9}{2} \left(\frac{G}{M_*}\right)^{1/2} \frac{R_*^5 M_p}{Q_*} a^{-13/2}, \end{aligned} \quad (8)$$

$$\begin{aligned} \frac{1}{e} \frac{de}{dt} &= -\frac{63}{4} (GM_*^3)^{1/2} \frac{R_p^5}{Q_p M_p} a^{-13/2} \\ &\quad + \frac{171}{16} \left(\frac{G}{M_*}\right)^{1/2} \frac{R_*^5 M_p}{Q_*} a^{-13/2}. \end{aligned} \quad (9)$$

In order to determine the evolution of semi-major axis a and orbital eccentricity e numerically from Eq.(8) and Eq.(9), we

need to set the values of stellar dissipation parameter Q_* and planetary dissipation parameter Q_p . As mentioned in Essick and Weinberg (2016), the value of parameter Q_* also depends on the shape of orbit and the mass of companion. It is related to energy dissipation through heat and waves generated by tidal forces. For solar-type binary stars, it is about 10^6 (Meibom and Mathieu, 2005). For hot Jupiters, Essick and Weinberg (2016) suggested the value of Q_* to be about $10^5 \sim 10^6$ but Matsumura et al. (2010) considered a larger range as $10^4 \sim 10^9$. As for the planetary dissipation parameter Q_p , Trilling et al. (2000) suggested a value $Q_p = 10^5$, but Jackson et al. (2008) gave $Q_p = 10^{6.5}$.

To show the effect of different values of the parameters Q_* and Q_p , we set two values of Q_* , i.e. 10^4 and 10^9 , and three values of Q_p , i.e. 10^5 , 10^6 , $10^{6.5}$. With these values, Eq.(8)-(9) are integrated backward in time (Jackson et al., 2008) and the results are presented in Fig.4. There are six cases in each panel, in which different marks are for different Q_* values and different colors are for different Q_p values. That is, circles are for $Q_* = 10^4$; curves are for $Q_* = 10^9$; the green color is for $Q_p = 10^5$; the blue color is for $Q_p = 10^6$; the black color is for $Q_p = 10^{6.5}$.

The horizontal axes show the backward time with $t = 0$ for the current time. Considering the evolution backward in time, the semi-major axis a and eccentricity e increase quickly from $t = 0$ to $t = -0.1$ Gyrs and then increase slowly for both HAT-P-51b and HAT-P-53b. We can also find that the result of HAT-P-51b does not really depend on the values of Q_* . The result is mainly influenced by the values of Q_p . However, the result of HAT-P-53b are influenced by both Q_* and Q_p .

It is obvious that the eccentricity goes beyond $e = 1$ for many cases, which are unlikely to be physical. For HAT-P-51b, the cases with $Q_p = 10^6$ and $Q_p = 10^{6.5}$ are physical. For HAT-P-53b, only when $Q_* = 10^9$, the cases with $Q_p = 10^6$ and $Q_p = 10^{6.5}$ are physical. Ignoring those parts of evolution with eccentricity beyond $e = 1$, we can collect the results within $0 < e < 1$ of all six cases for both HAT-P-51b and HAT-P-53b and see the evolution on the $a - e$ plane, as presented in Fig.5. These theoretical models show that the semi-major axis a and eccentricity e would continue to decrease monotonically in the future.

5. Conclusions

The transit observations continuously make contributions to the exoplanet research. It does not only bring the discoveries of new systems, but also characterize their orbital evolution. The presented observational results here are directly derived from the combination of Kepler Catalog (Holczer et al., 2016), TESS Catalog (Ivshina and Winn, 2022), and ExoClock Catalog (Kokori et al., 2023). This combination forms the most complete database up to date. In order to focus on those exoplanets which could be influenced by the star-planet tidal interactions, the planets with orbital period $p < 10$ days and planetary mass $m > 0.3$ Jupiter-Mass are picked as hot Jupiters. After performing the data-model fitting with both fixed-orbit

Name	$M_p(M_J)$	$a(AU)$	$M_*(M_\odot)$	$R_*(R_\odot)$	e
HAT-P-51b	0.309	0.05069	0.976	1.041	0.123
HAT-P-53b	1.487	0.03159	1.093	1.209	0.134
TrES-5b	1.778	0.02446	0.893	0.866	0 ^[a]
WASP-12b	1.47	0.02344	1.434	1.657	0

Table 4: The planetary mass, planetary orbital semi-major axis, star’s mass, star’s radius, and planetary orbital eccentricity for planets belonging to the orbit-decay-TTV type. These parameters are adopted from *The Extrasolar Planets Encyclopaedia* <http://exoplanet.eu/>. Note [a] : This eccentricity value is from Mandushev et al. (2011).

Name	Q_*	LQ_*	UQ_*
HAT-P-51b	-	-	-
HAT-P-53b	-	-	-
TrES-5b	$9619.98^{+740.04}_{-645.92}$	8412.426	12324.42
WASP-12b	$165140.76^{+4134.33}_{-3930.96}$	157452.63	178548.32

Table 5: The best-fit stellar dissipation parameter Q_* , its lower limit LQ_* , and upper limit UQ_* for planets belonging to the orbit-decay-TTV type. Note that there are no determined values for HAT-P-51b and HAT-P-53b as their eccentricities are not zero.

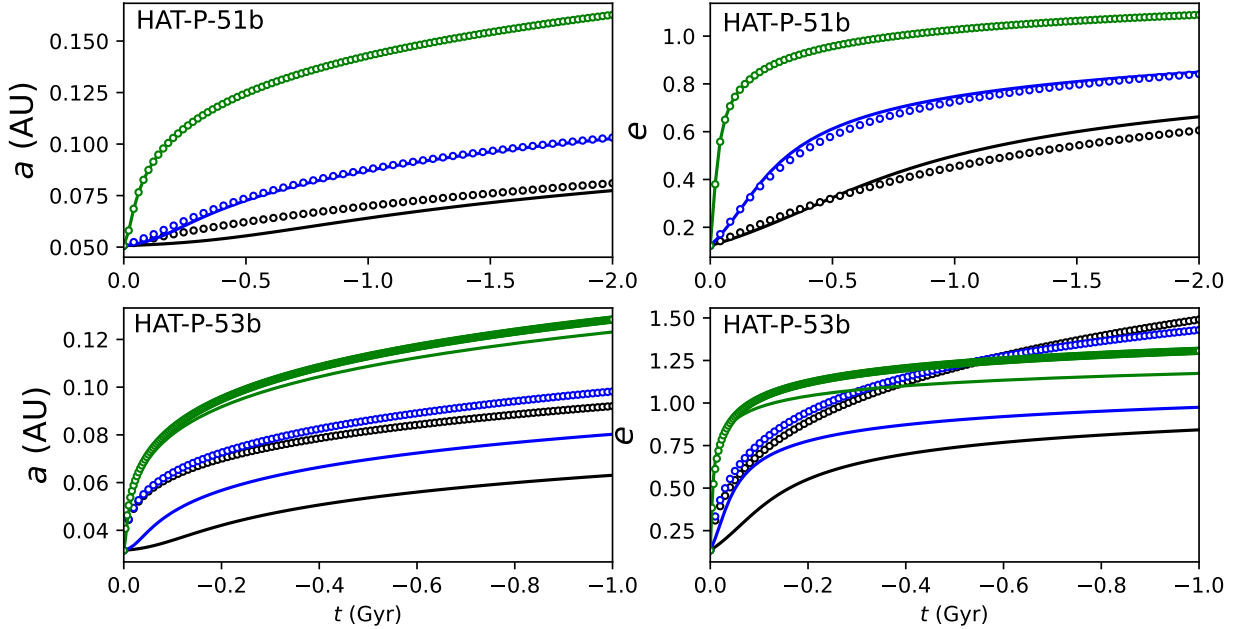


Figure 4: The semi-major axis a and eccentricity e as functions of the backward time for HAT-P-51b and HAT-P-53b. In each panel, circles are for $Q_* = 10^4$; curves are for $Q_* = 10^9$; the green color is for $Q_p = 10^5$; the blue color is for $Q_p = 10^6$; the black color is for $Q_p = 10^{6.5}$.

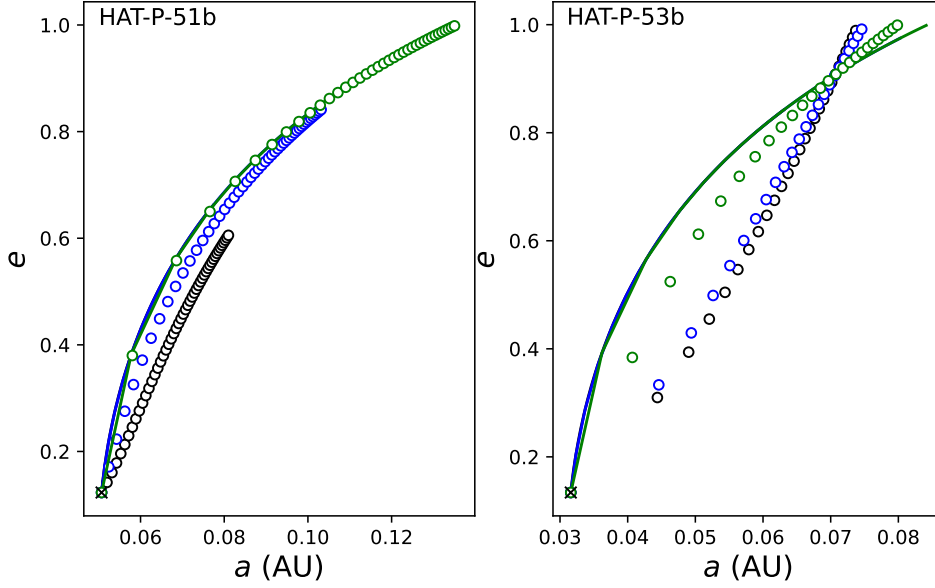


Figure 5: The orbital evolution on the $a - e$ plane for HAT-P-51b and HAT-P-53b. In each panel, circles are for $Q_* = 10^4$; curves are for $Q_* = 10^9$; the green color is for $Q_p = 10^5$; the blue color is for $Q_p = 10^6$; the black color is for $Q_p = 10^{6.5}$. The crosses indicate the current values of semi-major axis a and eccentricity e .

and orbit-decay models, only those with best-fit $dP_v/dN < 0$ become the sample planets here.

Among these 144 planets, 118 are classified as the null-TTV type, 22 belong to the unclassified-TTV type, and 4 are classified as the orbit-decay-TTV type. Explicitly, HAT-P-51b, HAT-P-53b, TrES-5b, WASP-12b are the orbit-decay cases. Therefore, our results reconfirm that WASP-12b is an orbit-decay planet, and also show that HAT-P-51b, HAT-P-53b, TrES-5b are potential orbit-decay candidates. Apparently, future observational data would be very helpful to reveal the orbital nature of HAT-P-51b, HAT-P-53b, TrES-5b, as well as those 22 unclassified-TTV-type planets.

Acknowledgements

We are grateful to the anonymous referee for good suggestions, which help to improve this paper significantly. This project is supported in part by the National Science and Technology Council, Taiwan, under Li-Chin Yeh's Grant MOST 111-2115-M-007-008 and Ing-Guey Jiang's Grant MOST 111-2112-M-007-035.

References

A-thano, N., Jiang, I.G., Awiphan, S., Rattanamala, R., Su, L.H., Hengpiya, T., Sariya, D.P., Yeh, L.C., Shlyapnikov, A.A., Gorbachev, M.A., Rublevski, A.N., Mannaday, V.K., Thakur, P., Sahu, D.K., Mkrtychian, D., Griv, E., 2022. The Transit Timing and Atmosphere of Hot Jupiter HAT-P-37b. *AJ* 163, 77. doi:10.3847/1538-3881/ac416d, arXiv:2112.04724.

Alonso, R., Brown, T.M., Torres, G., Latham, D.W., Sozzetti, A., Mandushev, G., Belmonte, J.A., Charbonneau, D., Deeg, H.J., Dunham, E.W., O'Donovan, F.T., Stefanik, R.P., 2004. TrES-1: The Transiting Planet of a Bright K0 V Star. *ApJ* 613, L153–L156. doi:10.1086/425256, arXiv:astro-ph/0408421.

Auvergne, M., Bodin, P., Boisdard, L., Buey, J.T., Chaintreuil, S., Epstein, G., Joutet, M., Lam-Trong, T., Levacher, P., Magnan, A., Perez, R., Plasson, P., Plessier, J., Peter, G., Steller, M., Tiphène, D., Baglin, A., Agogue, P., Appourchaux, T., Barbet, D., Beaufort, T., Bellenger, R., Berlin, R., Bernardi, P., Blouin, D., Boumier, P., Bonneau, F., Briet, R., Butler, B., Cautain, R., Chiavassa, F., Costes, V., Cuvillo, J., Cunha-Parro, V., de Oliveira Fialho, F., Decaudin, M., Defise, J.M., Djalal, S., Docclo, A., Drummond, R., Dupuis, O., Exil, G., Fauré, C., Gaboriaud, A., Gamet, P., Gavaldà, P., Grolleau, E., Gueguen, L., Guivarc'h, V., Guterman, P., Hasiba, J., Huntzinger, G., Hustaix, H., Imbert, C., Jeanville, G., Johlander, B., Jorda, L., Journoud, P., Karioty, F., Kerjean, L., Lafond, L., Lapeyrière, V., Landiech, P., Larqué, T., Laudet, P., Le Merrer, J., Leporati, L., Leruyet, B., Levieuge, B., Liebaria, A., Martin, L., Mazy, E., Mesnager, J.M., Michel, J.P., Moalic, J.P., Monjoin, W., Naudet, D., Neukirchner, S., Nguyen-Kim, K., Ollivier, M., Orcesi, J.L., Ottacher, H., Oulali, A., Parisot, J., Perruchot, S., Piacentino, A., Pinheiro da Silva, L., Platzer, J., Pontet, B., Pradines, A., Quentin, C., Rohbeck, U., Rolland, G., Rollenhagen, F., Romagnan, R., Russ, N., Samadi, R., Schmidt, R., Schwartz, N., Sebbag, I., Smit, H., Sunter, W., Tello, M., Toulouse, P., Ulmer, B., Vandermarcq, O., Vergnault, E., Wallner, R., Wautier, G., Zanatta, P., 2009. The CoRoT satellite in flight: description and performance. *A&A* 506, 411–424. doi:10.1051/0004-6361/200810860, arXiv:0901.2206.

Bakos, G., Noyes, R.W., Kovács, G., Stanek, K.Z., Sasselov, D.D., Domsa, I., 2004. Wide-Field Millimagitude Photometry with the HAT: A Tool for Extrasolar Planet Detection. *PASP* 116, 266–277. doi:10.1086/382735, arXiv:astro-ph/0401219.

Barclay, T., Pepper, J., Quintana, E.V., 2018. A Revised Exoplanet Yield from the Transiting Exoplanet Survey Satellite (TESS). *ApJS* 239, 2. doi:10.3847/1538-4365/aae3e9, arXiv:1804.05050.

Barros, S.C.C., Akasani, B., Boué, G., Smith, A.M.S., Laskar, J., Ulmer-Moll, S., Lillo-Box, J., Queloz, D., Cameron, A.C., Sousa, S.G., Ehrenreich, D., Hooton, M.J., Bruno, G., Demory, B.O., Correia, A.C.M., Demangeon, O.D.S., Wilson, T.G., Bonfanti, A., Hoyer, S., Alibert, Y., Alonso, R., Escudé, G.A., Barbato, D., Bérczy, T., Barrado, D., Baumjohann, W., Beck, M., Beck, T., Benz, W., Bergomi, M., Billot, N., Bonfils, X., Bouchy, F., Brandeker, A., Broeg, C., Cabrera, J., Cessa, V., Charnoz, S., Damme, C.C.V., Davies, M.B., Deleuil, M., Deline, A., Delrez, L., Erikson, A., Fortier, A., Fossati, L., Fridlund, M., Gandolfi, D., Muñoz, A.G., Gillon, M., Güdel, M., Isaak, K.G., Heng, K., Kiss, L., des Etangs, A.L., Lendl,

- M., Lovis, C., Magrin, D., Nascimbeni, V., Macted, P.F.L., Olofsson, G., Ottensamer, R., Pagano, I., Pallé, E., Parviainen, H., Peter, G., Piotto, G., Pollacco, D., Ragazzoni, R., Rando, N., Rauer, H., Ribas, I., Santos, N.C., Scandariato, G., Ségransan, D., Simon, A.E., Steller, M., Szabó, G.M., Thomas, N., Udry, S., Ulmer, B., Van Grootel, V., Walton, N.A., 2022. Detection of the tidal deformation of WASP-103b at 3σ with CHEOPS. *A&A* 657, A52. doi:10.1051/0004-6361/202142196, arXiv:2201.03328.
- Blecic, J., Harrington, J., Madhusudhan, N., Stevenson, K.B., Hardy, R.A., Cubillos, P.E., Hardin, M., Bowman, O., Nymeyer, S., Anderson, D.R., Hellier, C., Smith, A.M.S., Collier Cameron, A., 2014. Spitzer Observations of the Thermal Emission from WASP-43b. *ApJ* 781, 116. doi:10.1088/0004-637X/781/2/116, arXiv:1302.7003.
- Borucki, W.J., Koch, D., Basri, G., Batalha, N., Brown, T., Caldwell, D., Caldwell, J., Christensen-Dalsgaard, J., Cochran, W.D., DeVore, E., Dunham, E.W., Dupree, A.K., Gautier, T.N., Geary, J.C., Gilliland, R., Gould, A., Howell, S.B., Jenkins, J.M., Kondo, Y., Latham, D.W., Marcy, G.W., Meibom, S., Kjeldsen, H., Lissauer, J.J., Monet, D.G., Morrison, D., Saselov, D., Tarter, J., Boss, A., Brownlee, D., Owen, T., Buzasi, D., Charbonneau, D., Doyle, L., Fortney, J., Ford, E.B., Holman, M.J., Seager, S., Steffen, J.H., Welsh, W.F., Rowe, J., Anderson, H., Buchhave, L., Ciardi, D., Walkowicz, L., Sherry, W., Horch, E., Isaacson, H., Everett, M.E., Fischer, D., Torres, G., Johnson, J.A., Endl, M., MacQueen, P., Bryson, S.T., Dotson, J., Haas, M., Kolodziejczak, J., Van Cleve, J., Chandrasekaran, H., Twicken, J.D., Quintana, E.V., Clarke, B.D., Allen, C., Li, J., Wu, H., Tenenbaum, P., Verner, E., Bruhweiler, F., Barnes, J., Prsa, A., 2010. Kepler Planet-Detection Mission: Introduction and First Results. *Science* 327, 977. doi:10.1126/science.1185402.
- Bouma, L.G., Winn, J.N., Baxter, C., Bhatti, W., Dai, F., Daylan, T., Désert, J.M., Hill, M.L., Kane, S.R., Stassun, K.G., Villaseñor, J., Ricker, G.R., Vanderspek, R., Latham, D.W., Seager, S., Jenkins, J.M., Berta-Thompson, Z., Colón, K., Fausnaugh, M., Glidden, A., Guerrero, N., Rodriguez, J.E., Twicken, J.D., Wohler, B., 2019. WASP-4b Arrived Early for the TESS Mission. *AJ* 157, 217. doi:10.3847/1538-3881/ab189f, arXiv:1903.02573.
- Davoudi, F., Baştürk, Ö., Yalçınkaya, S., Esmer, E.M., Safari, H., 2021. Investigation of Orbital Decay and Global Modeling of the Planet WASP-43 b. *AJ* 162, 210. doi:10.3847/1538-3881/ac1baf, arXiv:2111.03346.
- Essick, R., Weinberg, N.N., 2016. Orbital Decay of Hot Jupiters Due to Nonlinear Tidal Dissipation within Solar-type Hosts. *ApJ* 816, 18. doi:10.3847/0004-637X/816/1/18, arXiv:1508.02763.
- Ford, E.B., Ragozzine, D., Rowe, J.F., Steffen, J.H., Barclay, T., Batalha, N.M., Borucki, W.J., Bryson, S.T., Caldwell, D.A., Fabrycky, D.C., Gautier, T.N., Holman, M.J., Ibrahim, K.A., Kjeldsen, H., Kinemuchi, K., Koch, D.G., Lissauer, J.J., Still, M., Tenenbaum, P., Uddin, K., Welsh, W., 2012. Transit Timing Observations from Kepler. V. Transit Timing Variation Candidates in the First Sixteen Months from Polynomial Models. *ApJ* 756, 185. doi:10.1088/0004-637X/756/2/185, arXiv:1201.1892.
- Foreman-Mackey, D., Hogg, D.W., Lang, D., Goodman, J., 2013. emcee: The MCMC Hammer. *PASP* 125, 306. doi:10.1086/670067, arXiv:1202.3665.
- Garai, Z., Pribulla, T., Parviainen, H., Pallé, E., Claret, A., Szigeti, L., Béjar, V.J.S., Casasayas-Barris, N., Crouzet, N., Fukui, A., Chen, G., Kawauchi, K., Klagyivik, P., Kurita, S., Kusakabe, N., de Leon, J.P., Livingston, J.H., Luque, R., Mori, M., Murgas, F., Narita, N., Nishiumi, T., Oshagh, M., Szabó, G.M., Tamura, M., Terada, Y., Watanabe, N., 2021. Is the orbit of the exoplanet WASP-43b really decaying? TESS and MuSCAT2 observations confirm no detection. *MNRAS* 508, 5514–5523. doi:10.1093/mnras/stab2929, arXiv:2110.04761.
- Goldreich, P., Soter, S., 1966. Q in the Solar System. *Icarus* 5, 375–389. doi:10.1016/0019-1035(66)90051-0.
- Goodman, J., Weare, J., 2010. Ensemble samplers with affine invariance. *Communications in Applied Mathematics and Computational Science* 5, 65–80. doi:10.2140/camcos.2010.5.65.
- Hagey, S.R., Edwards, B., Boley, A.C., 2022. Evidence of Long-term Period Variations in the Exoplanet Transit Database (ETD). *AJ* 164, 220. doi:10.3847/1538-3881/ac959a, arXiv:2209.10752.
- Hartman, J.D., Bhatti, W., Bakos, G.Á., Bieryla, A., Kovács, G., Latham, D.W., Csabry, Z., de Val-Borro, M., Penev, K., Buchhave, L.A., Torres, G., Howard, A.W., Marcy, G.W., Johnson, J.A., Isaacson, H., Sato, B., Boisse, I., Falco, E., Everett, M.E., Szklenar, T., Fulton, B.J., Shporer, A., Kovács, T., Hansen, T., Béky, B., Noyes, R.W., Lázár, J., Papp, I., Sári, P., 2015. HAT-P-50b, HAT-P-51b, HAT-P-52b, and HAT-P-53b: Three Transiting Hot Jupiters and a Transiting Hot Saturn From the HATNet Survey. *AJ* 150, 168. doi:10.1088/0004-6256/150/6/168, arXiv:1503.04149.
- Hellier, C., Anderson, D.R., Collier Cameron, A., Gillon, M., Jehin, E., Lendl, M., Macted, P.F.L., Pepe, F., Pollacco, D., Queloz, D., Ségransan, D., Smalley, B., Smith, A.M.S., Southworth, J., Triard, A.H.M.J., Udry, S., West, R.G., 2011. WASP-43b: the closest-orbiting hot Jupiter. *A&A* 535, L7. doi:10.1051/0004-6361/201117081, arXiv:1104.2823.
- Hogg, R.V., Craig, A.T., 1989. Introduction to Mathematical Statistics. Macmillan Publishing Company, New York.
- Holczer, T., Mazeh, T., Nachmani, G., Jontof-Hutter, D., Ford, E.B., Fabrycky, D., Ragozzine, D., Kane, M., Steffen, J.H., 2016. Transit Timing Observations from Kepler. IX. Catalog of the Full Long-cadence Data Set. *ApJS* 225, 9. doi:10.3847/0067-0049/225/1/9, arXiv:1606.01744.
- Hoyer, S., Pallé, E., Dragomir, D., Murgas, F., 2016. Ruling out the Orbital Decay of the WASP-43b Exoplanet. *AJ* 151, 137. doi:10.3847/0004-6256/151/6/137, arXiv:1603.01144.
- Ivshina, E.S., Winn, J.N., 2022. TESS Transit Timing of Hundreds of Hot Jupiters. *ApJS* 259, 62. doi:10.3847/1538-4365/ac545b, arXiv:2202.03401.
- Jackson, B., Greenberg, R., Barnes, R., 2008. Tidal Evolution of Close-in Extrasolar Planets. *ApJ* 678, 1396–1406. doi:10.1086/529187, arXiv:0802.1543.
- Jackson, B., Jensen, E., Peacock, S., Arras, P., Penev, K., 2016. Tidal decay and stable Roche-lobe overflow of short-period gaseous exoplanets. *Celestial Mechanics and Dynamical Astronomy* 126, 227–248. doi:10.1007/s10569-016-9704-1, arXiv:1603.00392.
- Jiang, I.G., Ip, W.H., Yeh, L.C., 2003. On the Fate of Close-in Extrasolar Planets. *ApJ* 582, 449–454. doi:10.1086/344590, arXiv:astro-ph/0209061.
- Jiang, I.G., Lai, C.Y., Savushkin, A., Mkrtichian, D., Antonyuk, K., Griv, E., Hsieh, H.F., Yeh, L.C., 2016. The Possible Orbital Decay and Transit Timing Variations of the Planet WASP-43b. *AJ* 151, 17. doi:10.3847/0004-6256/151/1/17, arXiv:1511.00768.
- Jiang, I.G., Yeh, L.C., Chang, Y.C., Hung, W.L., 2007. On the Mass-Period Distributions and Correlations of Extrasolar Planets. *AJ* 134, 2061–2066. doi:10.1086/522888, arXiv:0709.0578.
- Jiang, I.G., Yeh, L.C., Thakur, P., Wu, Y.T., Chien, P., Lin, Y.L., Chen, H.Y., Hu, J.H., Sun, Z., Ji, J., 2013. Possible Transit Timing Variations of the TrES-3 Planetary System. *AJ* 145, 68. doi:10.1088/0004-6256/145/3/68, arXiv:1308.2456.
- Kipping, D., Yahalomi, D.A., 2023. A search for transit timing variations within the exomoon corridor using Kepler data. *MNRAS* 518, 3482–3493. doi:10.1093/mnras/stac3360, arXiv:2211.06210.
- Kokori, A., Tsiaras, A., Edwards, B., Jones, A., Pantelidou, G., Tinetti, G., Bewersdorff, L., Iliadou, A., Jongen, Y., Lekkas, G., Nastasi, A., Poul-tourtzidis, E., Sidiropoulos, C., Walter, F., Wünsche, A., Abraham, R., Agnihotri, V.K., Albanesi, R., Arce-Mansego, E., Arnot, D., Audejean, M., Aumasson, C., Bachschmidt, M., Baj, G., Barroy, P.R., Belinski, A.A., Bennett, D., Benni, P., Bernacki, K., Betti, L., Biagini, A., Bosch, P., Brandebourg, P., Brát, L., Bretton, M., Brincat, S.M., Brouillard, S., Bruzas, A., Bruzzone, A., Buckland, R.A., Caló, M., Campos, F., Carreño, A., Carrion Rodrigo, J.A., Casali, R., Casalnuovo, G., Cataneo, M., Chang, C.M., Changeat, L., Chowdhury, V., Ciantini, R., Cilluffo, M., Coliac, J.F., Conzo, G., Correa, M., Coulon, G., Crouzet, N., Crow, M.V., Curtis, I.A., Daniel, D., Dauchet, B., Dawes, S., Deldem, M., Deligeorgopoulos, D., Dransfield, G., Dymock, R., Eenmäe, T., Esseiva, N., Evans, P., Falco, C., Farfán, R.G., Fernández-Lajús, E., Ferratfiat, S., Ferreira, S.L., Ferretti, A., Fiolka, J., Fowler, M., Futcher, S.R., Gabellini, D., Gainey, T., Gaitan, J., Gajdoš, P., García-Sánchez, A., Garlitz, J., Gillier, C., Gison, C., Gonzales, J., Gorshanov, D., Grau Horta, F., Grivas, G., Guerra, P., Guillot, T., Haswell, C.A., Haymes, T., Hentunen, V.P., Hills, K., Hose, K., Humbert, T., Hurter, F., Hynek, T., Iryzk, M., Jacobsen, J., Jannetta, A.L., Johnson, K., Jóźwik-Wabik, P., Krzouach, A.E., Kang, W., Kiiskinen, H., Kim, T., Kivila, Ü., Koch, B., Kolb, U., Kučáková, H., Lai, S.P., Laloum, D., Lasota, S., Lewis, L.A., Liakos, G.I., Libotte, F., Lomoz, F., Lopresti, C., Majewski, R., Malcher, A., Mallonn, M., Mannucci, M., Marchini, A., Mari, J.M., Marino, A., Marino, G., Mario, J.C., Marquette, J.B., Martínez-Bravo, F.A., Mašek, M., Matassa, P., Michel, P., Michelet, J., Miller, M., Miny, E., Molina, D., Mollier, T., Monteleone, B., Montigiani, N., Morales-Aimar, M., Mortari, F., Morvan, M., Mugnai, L.V., Murawski, G., Naponiello, L., Naudin, J.L., Naves, R.,

- Néel, D., Neito, R., Neveu, S., Noschese, A., Ögmen, Y., Ohshima, O., Orbanic, Z., Pace, E.P., Pantacchini, C., Paschalis, N.I., Pereira, C., Peretto, I., Perroud, V., Phillips, M., Pintr, P., Pioppa, J.B., Plazas, J., Poelarends, A.J., Popowicz, A., Purcell, J., Quinn, N., Raetz, M., Rees, D., Regembal, F., Rocchetto, M., Rocci, P.F., Rockenbauer, M., Roth, R., Rousselot, L., Rubia, X., Ruocco, N., Russo, E., Salisbury, M., Salvaggio, F., Santos, A., Savage, J., Scaggiante, F., Sedita, D., Shadick, S., Silva, A.F., Sioulas, N., Školník, V., Smith, M., Smolka, M., Solmaz, A., Stanbury, N., Stouraitis, D., Tan, T.G., Theusner, M., Thurston, G., Tifner, F.P., Tomacelli, A., Tomatis, A., Trnka, J., Tylšar, M., Valeau, P., Vignes, J.P., Villa, A., Vives Sureda, A., Vora, K., Vrašťák, M., Walliang, D., Wenzel, B., Wright, D.E., Zambelli, R., Zhang, M., Zibar, M., 2023. ExoClock Project. III. 450 New Exoplanet Ephemerides from Ground and Space Observations. *ApJS* 265, 4. doi:10.3847/1538-4365/ac9da4, arXiv:2209.09673.
- Kokori, A., Tsiaras, A., Edwards, B., Rocchetto, M., Tinetti, G., Bewersdorff, L., Jongen, Y., Lekkas, G., Pantelidou, G., Poulourtzidis, E., Wünsche, A., Aggelis, C., Agnihotri, V.K., Arena, C., Bachschmidt, M., Bennett, D., Benni, P., Bernacki, K., Besson, E., Betti, L., Biagini, A., Brandebourg, P., Bretton, M., Brincat, S.M., Caló, M., Campos, F., Casali, R., Ciantini, R., Crow, M.V., Dauchet, B., Dawes, S., Deldem, M., Deligeorgopoulos, D., Dymock, R., Eenmäe, T., Evans, P., Esseiva, N., Falco, C., Ferratfiat, S., Fowler, M., Futcher, S.R., Gaitan, J., Horta, F.G., Guerra, P., Hurter, F., Jones, A., Kang, W., Kiiskinen, H., Kim, T., Laloum, D., Lee, R., Lomoz, F., Lopresti, C., Mallonn, M., Mannucci, M., Marino, A., Mario, J.C., Marquette, J.B., Michelet, J., Miller, M., Mollier, T., Molina, D., Montigiani, N., Mortari, F., Morvan, M., Mugnai, L.V., Naponiello, L., Nastasi, A., Neito, R., Pace, E., Papadeas, P., Paschalis, N., Pereira, C., Perroud, V., Phillips, M., Pintr, P., Pioppa, J.B., Popowicz, A., Raetz, M., Regembal, F., Rickard, K., Roberts, M., Rousselot, L., Rubia, X., Savage, J., Sedita, D., Shave-Wall, D., Sioulas, N., Školník, V., Smith, M., St-Gelais, D., Stouraitis, D., Strikis, I., Thurston, G., Tomacelli, A., Tomatis, A., Trevan, B., Valeau, P., Vignes, J.P., Vora, K., Vrašťák, M., Walter, F., Wenzel, B., Wright, D.E., Zibar, M., 2022. ExoClock Project. II. A Large-scale Integrated Study with 180 Updated Exoplanet Ephemerides. *ApJS* 258, 40. doi:10.3847/1538-4365/ac3a10, arXiv:2110.13863.
- Kokori, A., Tsiaras, A., Edwards, B., Rocchetto, M., Tinetti, G., Wünsche, A., Paschalis, N., Agnihotri, V.K., Bachschmidt, M., Bretton, M., Caines, H., Caló, M., Casali, R., Crow, M., Dawes, S., Deldem, M., Deligeorgopoulos, D., Dymock, R., Evans, P., Falco, C., Ferratfiat, S., Fowler, M., Futcher, S., Guerra, P., Hurter, F., Jones, A., Kang, W., Kim, T., Lee, R., Lopresti, C., Marino, A., Mallonn, M., Mortari, F., Morvan, M., Mugnai, L.V., Nastasi, A., Perroud, V., Pereira, C., Phillips, M., Pintr, P., Raetz, M., Regembal, F., Savage, J., Sedita, D., Sioulas, N., Strikis, I., Thurston, G., Tomacelli, A., Tomatis, A., 2021. ExoClock project: an open platform for monitoring the ephemerides of Ariel targets with contributions from the public. *Experimental Astronomy* doi:10.1007/s10686-020-09696-3, arXiv:2012.07478.
- Maciejewski, G., Dimitrov, D., Fernández, M., Sota, A., Nowak, G., Ohlert, J., Nikolov, G., Bukowiecki, L., Hinse, T.C., Pallé, E., Tingley, B., Kjurkchieva, D., Lee, J.W., Lee, C.U., 2016. Departure from the constant-period ephemeris for the transiting exoplanet WASP-12. *A&A* 588, L6. doi:10.1051/0004-6361/201628312, arXiv:1602.09055.
- Maciejewski, G., Fernández, M., Aceituno, F., Martín-Ruiz, S., Ohlert, J., Dimitrov, D., Szyszka, K., von Essen, C., Mugrauer, M., Bischoff, R., Michel, K.U., Mallonn, M., Stangret, M., Moździerski, D., 2018. Planet-Star Interactions with Precise Transit Timing. I. The Refined Orbital Decay Rate for WASP-12 b and Initial Constraints for HAT-P-23 b, KELT-1 b, KELT-16 b, WASP-33 b and WASP-103 b. *Acta Astron.* 68, 371–401. doi:10.32023/0001-5237/68.4.4, arXiv:1812.02438.
- Maciejewski, G., Fernández, M., Aceituno, F., Ramos, J.L., Dimitrov, D., Donchev, Z., Ohlert, J., 2021. Revisiting TrES-5 b: departure from a linear ephemeris instead of short-period transit timing variation. *A&A* 656, A88. doi:10.1051/0004-6361/202142424, arXiv:2110.14294.
- Mandushev, G., Quinn, S.N., Buchhave, L.A., Dunham, E.W., Rabus, M., Oetiker, B., Latham, D.W., Charbonneau, D., Brown, T.M., Belmonte, J.A., O'Donovan, F.T., 2011. TrES-5: A Massive Jupiter-sized Planet Transiting a Cool G Dwarf. *ApJ* 741, 114. doi:10.1088/0004-637X/741/2/114, arXiv:1108.3572.
- Mannaday, V.K., Thakur, P., Jiang, I.G., Sahu, D.K., Joshi, Y.C., Pandey, A.K., Joshi, S., Yadav, R.K., Su, L.H., Sariya, D.P., Yeh, L.C., Griv, E., Mkrtychian, D., Shlyapnikov, A., Moskvina, V., Ignatov, V., Vaňko, M., Püsküllü, Ç., 2020. Probing Transit Timing Variation and Its Possible Origin with 12 New Transits of TrES-3b. *AJ* 160, 47. doi:10.3847/1538-3881/ab9818, arXiv:2006.00599.
- Mannaday, V.K., Thakur, P., Southworth, J., Jiang, I.G., Sahu, D.K., Mancini, L., Vaňko, M., Kundra, E., Gajdoš, P., A-thano, N., Sariya, D.P., Yeh, L.C., Griv, E., Mkrtychian, D., Shlyapnikov, A., 2022. Revisiting the Transit Timing Variations in the TrES-3 and Qatar-1 Systems with TESS Data. *AJ* 164, 198. doi:10.3847/1538-3881/ac91c2, arXiv:2209.04080.
- Matsumura, S., Peale, S.J., Rasio, F.A., 2010. Tidal Evolution of Close-in Planets. *ApJ* 725, 1995–2016. doi:10.1088/0004-637X/725/2/1995, arXiv:1007.4785.
- Meibom, S., Mathieu, R.D., 2005. A Robust Measure of Tidal Circularization in Coeval Binary Populations: The Solar-Type Spectroscopic Binary Population in the Open Cluster M35. *ApJ* 620, 970–983. doi:10.1086/427082, arXiv:astro-ph/0412147.
- Miralda-Escudé, J., 2002. Orbital Perturbations of Transiting Planets: A Possible Method to Measure Stellar Quadrupoles and to Detect Earth-Mass Planets. *ApJ* 564, 1019–1023. doi:10.1086/324279, arXiv:astro-ph/0104034.
- Murray, C.D., Dermott, S.F., 1999. *Solar System Dynamics*. Cambridge University Press, Cambridge.
- Pascale, E., Bezawada, N., Barstow, J., Beaulieu, J.P., Bowles, N., Coudé du Foresto, V., Coustenis, A., Decin, L., Drossart, P., Eccleston, P., Encrenaz, T., Forget, F., Griffin, M., Güdel, M., Hartogh, P., Heske, A., Lagage, P.O., Leconte, J., Malaguti, P., Micela, G., Middleton, K., Min, M., Moneti, A., Morales, J.C., Mugnai, L., Ollivier, M., Pace, E., Papageorgiou, A., Pilbratt, G., Puig, L., Rataj, M., Ray, T., Ribas, I., Rocchetto, M., Sarkar, S., Selsis, F., Taylor, W., Tennyson, J., Tinetti, G., Turrini, D., Vandenbussche, B., Venot, O., Waldmann, I.P., Wolkenberg, P., Wright, G., Zapatero Osorio, M.R., Zingales, T., 2018. The ARIEL space mission, in: Lystrup, M., MacEwen, H.A., Fazio, G.G., Batalha, N., Siegler, N., Tong, E.C. (Eds.), *Space Telescopes and Instrumentation 2018: Optical, Infrared, and Millimeter Wave*, p. 106980H. doi:10.1117/12.2311838.
- Patra, K.C., Winn, J.N., Holman, M.J., Yu, L., Deming, D., Dai, F., 2017. The Apparently Decaying Orbit of WASP-12b. *AJ* 154, 4. doi:10.3847/1538-3881/aa6d75, arXiv:1703.06582.
- Penev, K., Bouma, L.G., Winn, J.N., Hartman, J.D., 2018. Empirical Tidal Dissipation in Exoplanet Hosts From Tidal Spin-up. *AJ* 155, 165. doi:10.3847/1538-3881/aaaf71, arXiv:1802.05269.
- Poddany, S., Brát, L., Pejcha, O., 2010. Exoplanet Transit Database. Reduction and processing of the photometric data of exoplanet transits. *New Astronomy* 15, 297–301. doi:10.1016/j.newast.2009.09.001, arXiv:0909.2548.
- Pollacco, D.L., Skillen, I., Collier Cameron, A., Christian, D.J., Hellier, C., Irwin, J., Lister, T.A., Street, R.A., West, R.G., Anderson, D.R., Clarkson, W.I., Deeg, H., Enoch, B., Evans, A., Fitzsimmons, A., Haswell, C.A., Hodgkin, S., Horne, K., Kane, S.R., Keenan, F.P., Maxted, P.F.L., Norton, A.J., Osborne, J., Parley, N.R., Ryans, R.S.I., Smalley, B., Wheatley, P.J., Wilson, D.M., 2006. The WASP Project and the SuperWASP Cameras. *PASP* 118, 1407–1418. doi:10.1086/508556, arXiv:astro-ph/0608454.
- Press, W.H., Teukolsky, S.A., Vetterling, W.T., Flannery, B.P., 1992. *Numerical recipes in C. The art of scientific computing*. Cambridge University Press, Cambridge.
- Sokov, E.N., Sokova, I.A., Dyachenko, V.V., Rastegaev, D.A., Burdanov, A., Rusov, S.A., Benni, P., Shadick, S., Hentunen, V.P., Salisbury, M., Esseiva, N., Garlitz, J., Bretton, M., Ogmen, Y., Karavaev, Y., Ayiomamitis, A., Mazurenko, O., Alonso, D., Velichko, S.F., 2018. Transit timing analysis of the exoplanet TrES-5 b. Possible existence of the exoplanet TrES-5 c. *MNRAS* 480, 291–301. doi:10.1093/mnras/sty1615, arXiv:1806.03503.
- Steffen, J.H., Ford, E.B., Rowe, J.F., Fabrycky, D.C., Holman, M.J., Welsh, W.F., Batalha, N.M., Borucki, W.J., Bryson, S., Caldwell, D.A., Ciardi, D.R., Jenkins, J.M., Kjeldsen, H., Koch, D.G., Prša, A., Sanderfer, D.T., Seader, S., Twicken, J.D., 2012. Transit Timing Observations from Kepler. VI. Potentially Interesting Candidate Systems from Fourier-based Statistical Tests. *ApJ* 756, 186. doi:10.1088/0004-637X/756/2/186, arXiv:1201.1873.
- Su, L.H., Jiang, I.G., Sariya, D.P., Lee, C.Y., Yeh, L.C., Mannaday, V.K., Thakur, P., Sahu, D.K., Chand, S., Shlyapnikov, A.A., Moskvina, V.V., Ignatov, V., Mkrtychian, D., Griv, E., 2021. Are There Transit Timing Variations for the Exoplanet Qatar-1b? *AJ* 161, 108. doi:10.3847/1538-3881/

abd4d8, arXiv:2012.08184.

- Sun, L., Ioannidis, P., Gu, S., Schmitt, J.H.M.M., Wang, X., Kouwenhoven, M.B.N., 2019. Kepler-411: a four-planet system with an active host star. *A&A* 624, A15. doi:10.1051/0004-6361/201834275, arXiv:1902.09719.
- Szabó, G.M., Garai, Z., Brandeker, A., Gandolfi, D., Wilson, T.G., Deline, A., Olofsson, G., Fortier, A., Queloz, D., Borsato, L., Kiefer, F., Lecavelier des Etangs, A., Lendl, M., Serrano, L.M., Sulis, S., Ulmer Moll, S., Van Grootel, V., Alibert, Y., Alonso, R., Anglada, G., Bárczy, T., Barrado y Navascues, D., Barros, S.C.C., Baumjohann, W., Beck, M., Beck, T., Benz, W., Billot, N., Bonfanti, A., Bonfils, X., Broeg, C., Cabrera, J., Charnoz, S., Collier Cameron, A., Csizmadia, S., Davies, M.B., Deleuil, M., Delrez, L., Demangeon, O., Demory, B.O., Ehrenreich, D., Erikson, A., Fossati, L., Fridlund, M., Gillon, M., Güdel, M., Heng, K., Hoyer, S., Isaak, K.G., Kiss, L.L., Laskar, J., Lovis, C., Magrin, D., Maxted, P.F.L., Mecina, M., Nascimbeni, V., Ottensamer, R., Pagano, I., Pallé, E., Peter, G., Piotto, G., Pollacco, D., Ragazzoni, R., Rando, N., Rauer, H., Ribas, I., Santos, N.C., Sarajlic, M., Scandariato, G., Ségransan, D., Simon, A.E., Smith, A.M.S., Sousa, S.G., Steller, M., Thomas, N., Udry, S., Verrecchia, F., Walton, N., Wolter, D., 2022. Transit timing variations of AU Microscopii b and c. *A&A* 659, L7. doi:10.1051/0004-6361/202243076, arXiv:2202.04308.
- Trilling, D.E., Brown, R.H., Rivkin, A.S., 2000. Circumstellar Dust Disks around Stars with Known Planetary Companions. *ApJ* 529, 499–505. doi:10.1086/308280.
- Turner, J.D., Ridden-Harper, A., Jayawardhana, R., 2021. Decaying Orbit of the Hot Jupiter WASP-12b: Confirmation with TESS Observations. *AJ* 161, 72. doi:10.3847/1538-3881/abd178, arXiv:2012.02211.
- Valsecchi, F., Rappaport, S., Rasio, F.A., Marchant, P., Rogers, L.A., 2015. Tidally-driven Roche-lobe Overflow of Hot Jupiters with MESA. *ApJ* 813, 101. doi:10.1088/0004-637X/813/2/101, arXiv:1506.05175.
- Winn, J.N., Holman, M.J., Carter, J.A., Torres, G., Osip, D.J., Beatty, T., 2009. The Transit Light Curve Project. XI. Submillimagnitude Photometry of Two Transits of the Bloated Planet WASP-4b. *AJ* 137, 3826–3833. doi:10.1088/0004-6256/137/4/3826, arXiv:0901.4346.
- Wong, I., Shporer, A., Vissapragada, S., Greklek-McKeon, M., Knutson, H.A., Winn, J.N., Benneke, B., 2022. TESS Revisits WASP-12: Updated Orbital Decay Rate and Constraints on Atmospheric Variability. *AJ* 163, 175. doi:10.3847/1538-3881/ac5680, arXiv:2201.08370.
- Wu, D.H., Rice, M., Wang, S., 2023. Evidence for Hidden Nearby Companions to Hot Jupiters. *AJ* 165, 171. doi:10.3847/1538-3881/acbf3f, arXiv:2302.12778.
- Yee, S.W., Winn, J.N., Knutson, H.A., Patra, K.C., Vissapragada, S., Zhang, M.M., Holman, M.J., Shporer, A., Wright, J.T., 2020. The Orbit of WASP-12b Is Decaying. *ApJ* 888, L5. doi:10.3847/2041-8213/ab5c16, arXiv:1911.09131.
- Zhu, W., Wu, Y., 2018. The Super Earth-Cold Jupiter Relations. *AJ* 156, 92. doi:10.3847/1538-3881/aad22a, arXiv:1805.02660.